Journal of New Developments in Chemistry

Open Access - Peer-Reviewed - ISSN 2377-2549

Portico Archived | Crossref DOI | CC BY 4.0 Licensed

Research Article

Vibrational Spectral Analysis and First Order Hyperpolarizability Calculations on (E)-N′-(furan-2-yl methylene) Nicotinohydrazide

S. Bharanidharan [1], H. Saleem [1*], S. Subashchandrabose [2], M. Suresh [3], A. Nathiya [1], M. Syed Ali Padusha [4]

[1] Department of Physics, Annamalai University, Annamalainagar-608002, Tamil Nadu, India

[2] Centre for Research and Development, PRIST University, Thanjavur-613403, Tamil Nadu, India

[3] Department of Chemistry, L. N. Government College (Autonomous), Ponneri-601204, Tamil Nadu, India

[4] PG and Research Dept. of Chemistry, Jamal Mohamad College (Autonomous), Trichy 620020, Tamil Nadu, India

*** Correspondence:** Dr. H. Saleem, Department of Physics, Annamalai University, Annamalainagar-608002, Tamil Nadu, India (Dr. H. Saleem), Mobile: +91 9443879295

Published citation: S. Bharanidharan, H. Saleem, S. Subashchandrabose, M. Suresh, A. Nathiya et al. (2016) **Vibrational Spectral Analysis and First Order Hyperpolarizability Calculations on (E)-N′-(furan-2-yl methylene) Nicotinohydrazide**. *Journal of New Developments in Chemistry* - 1(2):1-26. https://doi.org/10.14302/issn.2377-2549.jndc-16-949

Article DOI: 10.14302/issn.2377-2549.jndc-16-949

Abstract

Vibrational spectral analysis and first order hyperpolarizability calculations on (E)-N′-(furan-2-ylmethylene) nicotinohydrazide (F2CNH), a novel, organic, hydrazone Schiff base compound was synthesized and its structure was characterized by FT-IR, FT-Raman and UV-visible spectrum. The optimized molecular structure, vibrational frequencies and corresponding vibrational assignments of F2CNH were performed on the basis of TED analysis using SQM method. Natural boding orbital (NBO) assessment has been carried out to clarify the charge transfer or conjugative interaction and delocalization of electron density within the molecule. Electronic transitions were studied employing UV-visible spectrum and the observed values were compared with theoretical values. The first order hyperpolarizability and related properties of F2NH were calculated. Besides FMO's MEP, mulliken atomic charge and various thermodynamic parameters such as Zero-point energy, rotational constant and enthalpy were also calculated and analyzed.

Keywords:
FT-IR; FT-Raman; TED; NBO; F2CNH;

Article Information	
Academic Editor	Zhe-Sheng Chenz, Professor Department of Pharmaceutical Sciences College of Pharmacy and Allied Health Professions St. John's University
Received Date	10 February 2016
Accepted Date	28 March 2016
Published Date	7 April 2016
Online	7 April 2016
Publication	Volume 1; Issue 2; Pages 1–26
Copyright	© 2016 Bharanidharan S, et al.
License	This is an open-access article distributed under the terms of the Creative Commons Attribution License, which permits unrestricted use, distribution, and reproduction in any medium, provided the original author and source are credited. https://creativecommons.org/licenses/by/4.0/

Introduction

Furan ring as an important group of heteroaromatic compounds that have been found in many natural products and substances that are useful in industrial applications [1]. It is often used as synthetic intermediates in the preparation of acyclic, carbocyclic, and heterocyclic compounds [2] and its derivatives as well as some other heterocyclic compounds are of great interest due to their application of molecules to characterise the active sites in zeolites [3], [4]. Furan is a heterocyclic organic compound consisting of a five member ring with one oxygen and four carbon atoms. Furan is a colorless, flammable, highly volatile liquid with a boiling point close to room temperature. Furan is found in heat-treated commercial foods and it is produced through thermal degradation of natural food constituents [5], [6]. Notably, it can be found in roasted coffee, instant coffee, and processed baby foods [7], [8]. Exposure to furan at doses about 2000 times the projected level of human exposure from foods increases the risk of hepatocellular tumors in rats and mice and bile duct tumors in rats [9] and thus furan is therefore listed as a possible human carcinogen [9].

The hydrazone derivatives in the organic molecule bring several physical and chemical properties. The hydrazones are bearing the >C=N-N< which leads the molecule towards nucleophilic and electrophilic nature. The ability of hydrazones to react with both electrophilic and nucleophilic reagents widens their application in organic chemistry and designing the new drugs [10], [11], [12]. Several hydrazone derivatives have been reported as insecticides, nematocides, herbicides, rodenticides and antituburculosis in addition to that some of the hydrazones were found to be active against leukemia, sarcoma and illnesses [10], [13].

Ramesh Babu et al., (2014) [14] reported the spectral Characterization of *(E)-1-(Furan-2-yl) methylene)-2-(1-phenylvinyl) hydrazine (FMPVH)* were carried out by using FT-IR, FT-Raman and UV–Vis spectrometry. The geometry, electronic properties, polarizability, and hyperpolarizability of *5-nitro-2-furaldehyde semicarbazone (5N2FSC)* have been calculated using density functional theory (DFT) with the hybrid functional B3LYP method by Vijay Narayan et al., 2011 [15]. In our previous study [16], investigation on "Structural and vibrational analysis of (E)-N'-(Pyridin-2-yl) methylene nicotinohydrazide" using Quantum chemical calculation have been carried out.

According to our knowledge, neither the quantum mechanical calculations nor the vibrational spectra of the title molecule F2CNH have been reported so far. Hence, in the present study, we aim to interpret the vibrational spectra of F2CNH molecule by applying the ab initio/DFT computations to derive information about vibrational frequencies, IR, Raman intensities, electronic transitions and intra-molecular charge transfer, etc.

Computational Details

The entire calculations were performed at DFT levels on a Pentium 1V/3.02 GHz personal computer using Gaussian 03W [17] program package, invoking gradient geometry optimization [17], [18]. In this study, the DFT/B3LYP/6-311++G(d,p) level of basis set was used for the computation of molecular structure, vibrational frequencies and energies of optimized structures. The vibrational modes were assigned on the basis of TED analysis using VEDA4 program [19].

It should be noted that Gaussian 03W package is able to calculate the Raman activity. The Raman activities were transformed into Raman intensities using Raint program [20] by the expression:

$$I_i = 10^{-12} \times (\nu_0 - \nu_i)^4 \times \frac{1}{\nu_i} \times RA_i \quad \textbf{(1)}$$

Where I_i is the Raman intensity, RA_i is the Raman scattering activities, ν_i is the wavenumber of the normal modes and ν_0 denotes the wavenumber of the excitation laser [21]. The same formula (Eqn. 1) has been used to convert the Raman activity into Raman intensity.

Experimental Details

Synthesis Procedure

10 mL of ethanolic solution of furfural (1 mL, 0.01 mol) was added to 5 mL of aqueous solution of nicotinic acid hydrazide (1.37 g, 0.01 mol) and stirred well for an hour in the presence of hydrochloric acid to form a white precipitate. The reaction mixture was maintained at room temperature and the colourless solid was obtained. The solid was separated and filtered under suction, washed with ice-cold water. The precipitate was washed with water and filtered and again washed with petroleum ether (40-60%) and dried over in a vacuum desiccator then the product was recrystallized from hot ethanol.

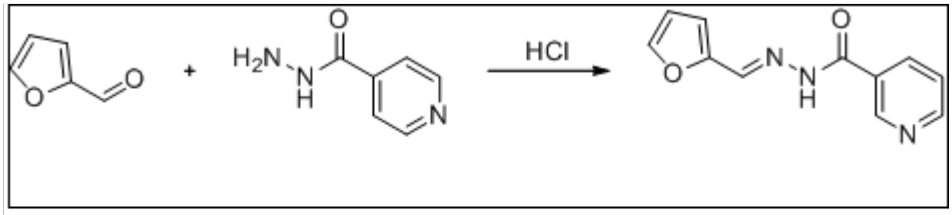

Results and Discussion

Molecular Geometry

The optimized bond parameters of F2CNH was carried out using DFT/B3LYP/6-311++G(d,p) basis set and are listed in Table 1. The optimized structure is shown in Figure 1. The title molecule consists of pyridin and furan rings linked by hydrazone linkage. The hydrazone linkage plays an important role in F2CNH. The electronic coupling between the amino hydrogen (N_{12}-H_{13}), carbonyl (C_{14}=O_{15}) lone-pair electrons and the (C_{14}-C_{16}) pyridine ring π-system creates phenyl N, O conjugations. These conjugations bring about intra-molecular charge (ICT) transfer. In the ICT state, the nπ interactions are substantially decreased, and thereby an electronic decoupling occurs from the ring π-system [22], which causes the differences in bond lengths of C_9=N_{11} (1.282Å), C_{14}-N_{12} (1.385Å) and also the variation of bond angles of C_{14}-C_{16}-C_{17} (117.59°) and C_{14}-C_{16}-C_{18} (123.59°). The bond distance of C_{14}-N_{12} is well below the single bond distance which indicates the electron delocalization over the region of the molecule and it is supported by literature [22].

 DOI: 10.14302/issn.2377-2549.jndc-16-949

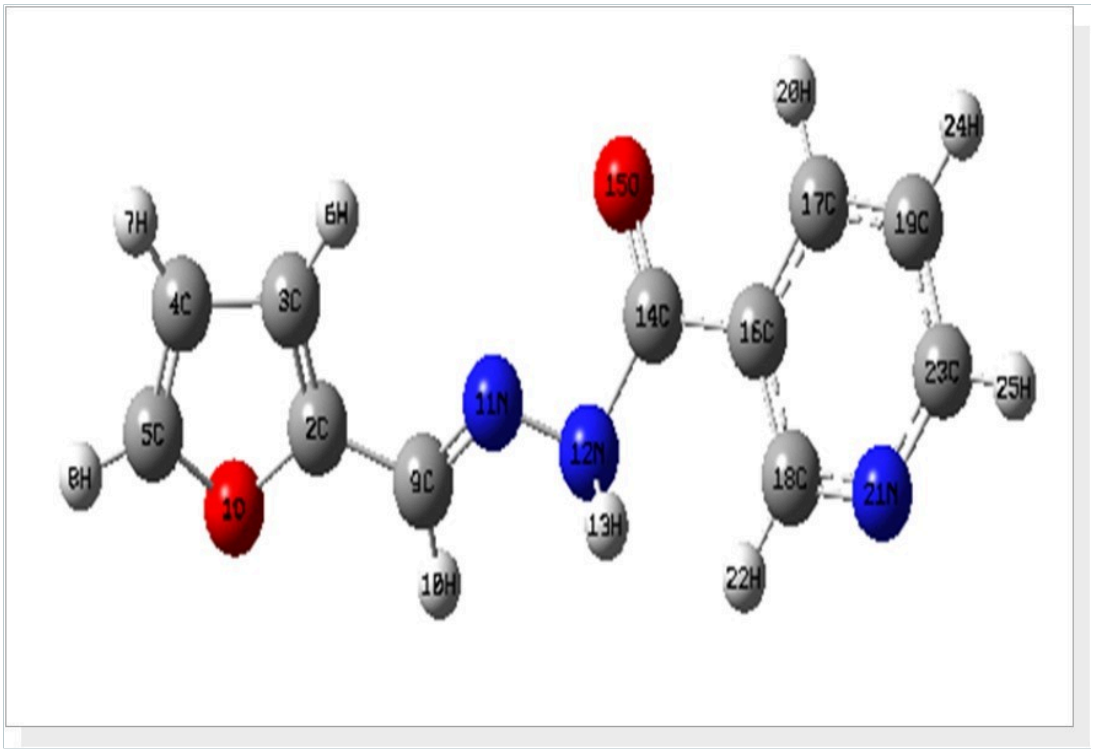

Figure 1. The optimized structure of (E)-N′-(furan-2-ylmethylene)nicotinohydrazide (F2CNH)

Table 1. The optimized bond parameters of F2CNH

Parametres	B3LYP/6-311++G(d,p)	XRD *
Bond Lengths (Å)		
O_1-C_2	1.372	1.366
O_1-C_5	1.358	1.368
C_2-C_3	1.369	1.348
C_2-C_9	1.441	1.432
C_3-C_4	1.425	1.415
C_3-H_6	1.077	0.930
C_4-C_5	1.362	1.368
C_4-H_7	1.078	0.930
C_5-H_8	1.076	0.930
C_9-N_{11}	1.282	1.273
N_{11}-N_{12}	1.356	1.384
N_{12}-H_{13}	1.015	0.860
N_{12}-C_{14}	1.385	1.348
C_{14}-O_{15}	1.212	1.230

 DOI: 10.14302/issn.2377-2549.jndc-16-949

Table 1 (continued)

Parametres	B3LYP/6-311++G(d,p)	XRD *
C_{14}-C_{16}	1.502	1.490
C_{16}-C_{17}	1.398	1.387
C_{16}-C_{18}	1.399	1.379
C_{17}-C_{19}	1.387	1.380
C_{17}-H_{20}	1.083	0.93
Bond Angles (°)		
O_1-C_2-C_3	109.67	110.11
O_1-C_2-C_9	115.72	119.36
C_3-C_2-C_9	134.59	130.51
C_2-C_3-C_4	106.38	106.54
C_2-C_3-H_6	125.49	126.70
C_4-C_3-H_6	128.11	126.7
C_3-C_4-C_5	106.40	106.65
C_3-C_4-H_7	127.33	126.70
C_5-C_4-H_7	126.25	126.7
O_1-C_5-C_4	110.45	111.01
O_1-C_5-H_8	115.96	124.5
C_4-C_5-H_8	133.58	124.5
C_2-C_9-H_{10}	116.03	119.10
C_2-C_9-N_{11}	121.14	121.81
H_{10}-C_9-N_{11}	122.81	119.10
C_9-N_{11}-N_{12}	116.86	116.43
N_{11}-N_{12}-H_{13}	119.33	120.40
N_{11}-N_{12}-C_{14}	121.07	119.16
H_{13}-N_{12}-C_{14}	119.31	120.4
N_{12}-C_{14}-O_{15}	123.61	122.65
Bond Angles (°)		
N_{12}-C_{14}-C_{16}	114.22	116.08
O_{15}-C_{14}-C_{16}	122.15	121.24
C_{14}-C_{16}-C_{17}	117.98	117.59
C_{14}-C_{16}-C_{18}	124.29	123.59

Table 1 (continued)

Parametres	B3LYP/6-311++G(d,p)	XRD *
C_{16}-C_{17}-C_{19}	118.94	118.82
C_{16}-C_{17}-H_{20}	119.08	119.9
C_{19}-C_{17}-H_{20}	121.96	119.9
C_{16}-C_{18}-H_{22}	120.92	120.39
C_{23}-C_{19}-H_{24}	120.27	120.01
C_{19}-C_{23}-H_{25}	120.52	120.0
Dihedral Angles (°)		
O_1-C_2-C_9-N_{11}	179.75	
C_3-C_2-C_9-H_{10}	179.90	
C_3-C_2-C_9-N_{11}	-0.20	
C_2-C_3-C_4-C_5	0.00	
C_2-C_3-C_4-H_7	179.99	
H_6-C_3-C_4-C_5	-179.98	
H_6-C_3-C_4-H_7	0.01	
C_3-C_4-C_5-O_1	-0.01	
C_3-C_4-C_5-H_8	179.99	
H_7-C_4-C_5-O_1	-180.00	
H_7-C_4-C_5-H_8	-0.00	
C_2-C_9-N_{11}-N_{12}	-179.48	
H_{10}-C_9-N_{11}-N_{12}	0.40	
C_9-N_{11}-N_{12}-H_{13}	-1.96	
C_9-N_{11}-N_{12}-C_{14}	-175.84	
N_{11}-N_{12}-C_{14}-O_{15}	2.95	
N_{11}-N_{12}-C_{14}-C_{16}	-177.75	
H_{13}-N_{12}-C_{14}-O_{15}	-170.92	
H_{13}-N_{12}-C_{14}-C_{16}	8.37	
N_{12}-C_{14}-C_{16}-C_{17}	-154.58	
N_{12}-C_{14}-C_{16}-C_{18}	28.13	
O_{15}-C_{14}-C_{16}-C_{17}	24.72	

* M.Z. Song, C.G. Fan, Acta Cryst. E 65 (2009) o2800

The bond angle of O_{15}=C_{14}-C_{16} is calculated at 121.24°, which is in agreement with literature value 122.15 and also finds support from literature Song and Fan, (2009) [23]. In hydrazone linkage, the angle

for C_9=N_{11}-N_{12} was calculated about 116.86° whereas the literature value is 116.43° [22]. The bond angles of C_{16}-C_{17}-H_{20} (119.09°) is negatively ~2.8° deviated from C_{19}-C_{17}-H_{20} (121.96°), which is due to the presence of O_{15} atom next to H_{20} atom. The furan ring moiety is planar [C_3-C_2-C_9-N_{11} = -0.20° and O_1-C_2-C_9-N_{11} = 179.75°] with hydrazone linkage, while phenyl ring is not planar [C_{17}-C_{16}-C_{14}-N_{12} = -154.58° and C_{18}-C_{16}-C_{14}-N_{12} = 28.13°]. Most of the calculated bond parameters are comparable with XRD values and also find support from the literature values of related structure [[24], [25]].

Vibrational Analysis

The fundamental vibrations of a non-linear molecule which contains N atoms is equal to (3N-6), apart from three translational and three rotational degrees of freedom [26], [27]. The F2CNH molecule

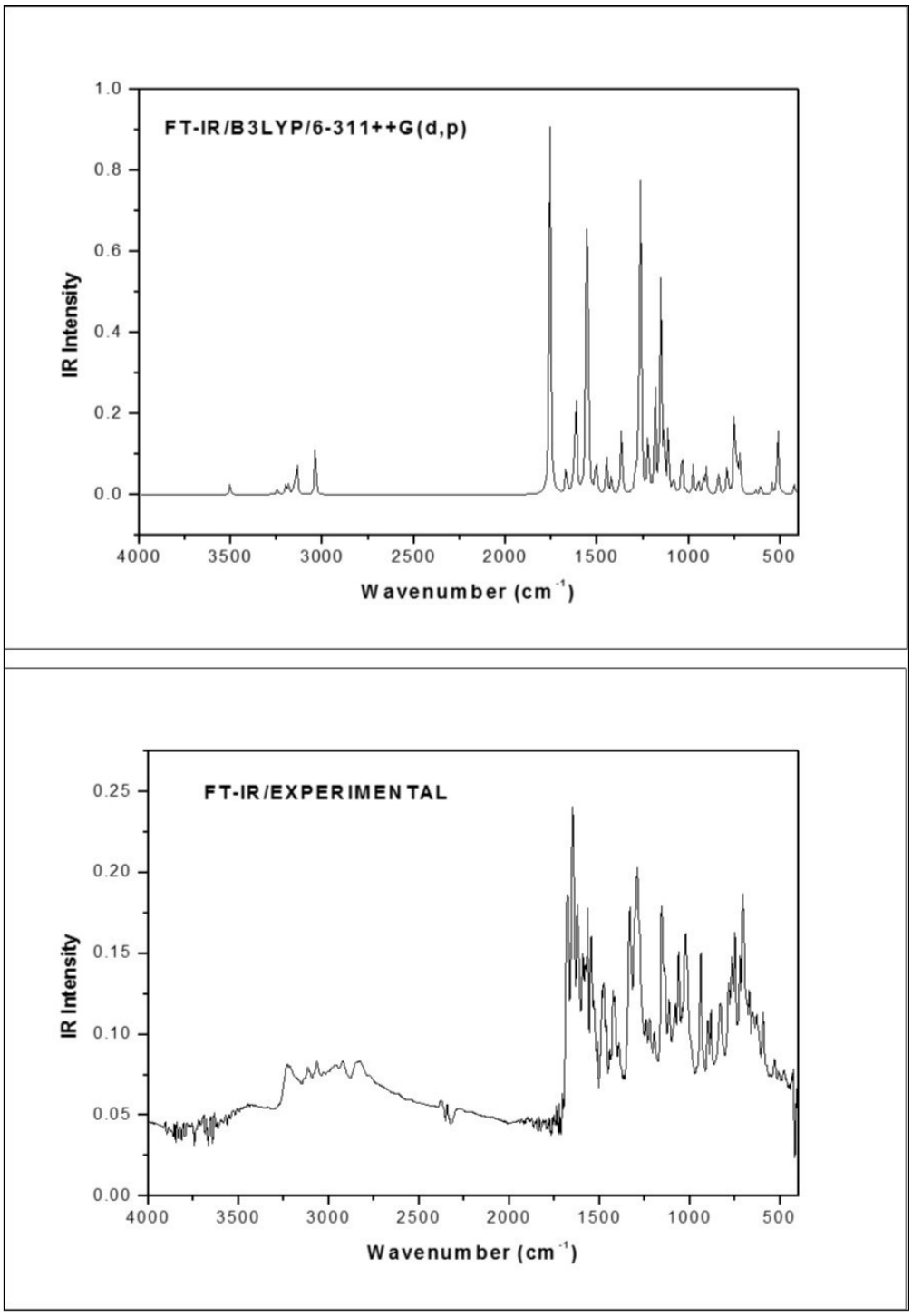

Figure 2. The Theoretical and Experimental FT-IR spectra of F2CNH

DOI: 10.14302/issn.2377-2549.jndc-16-949

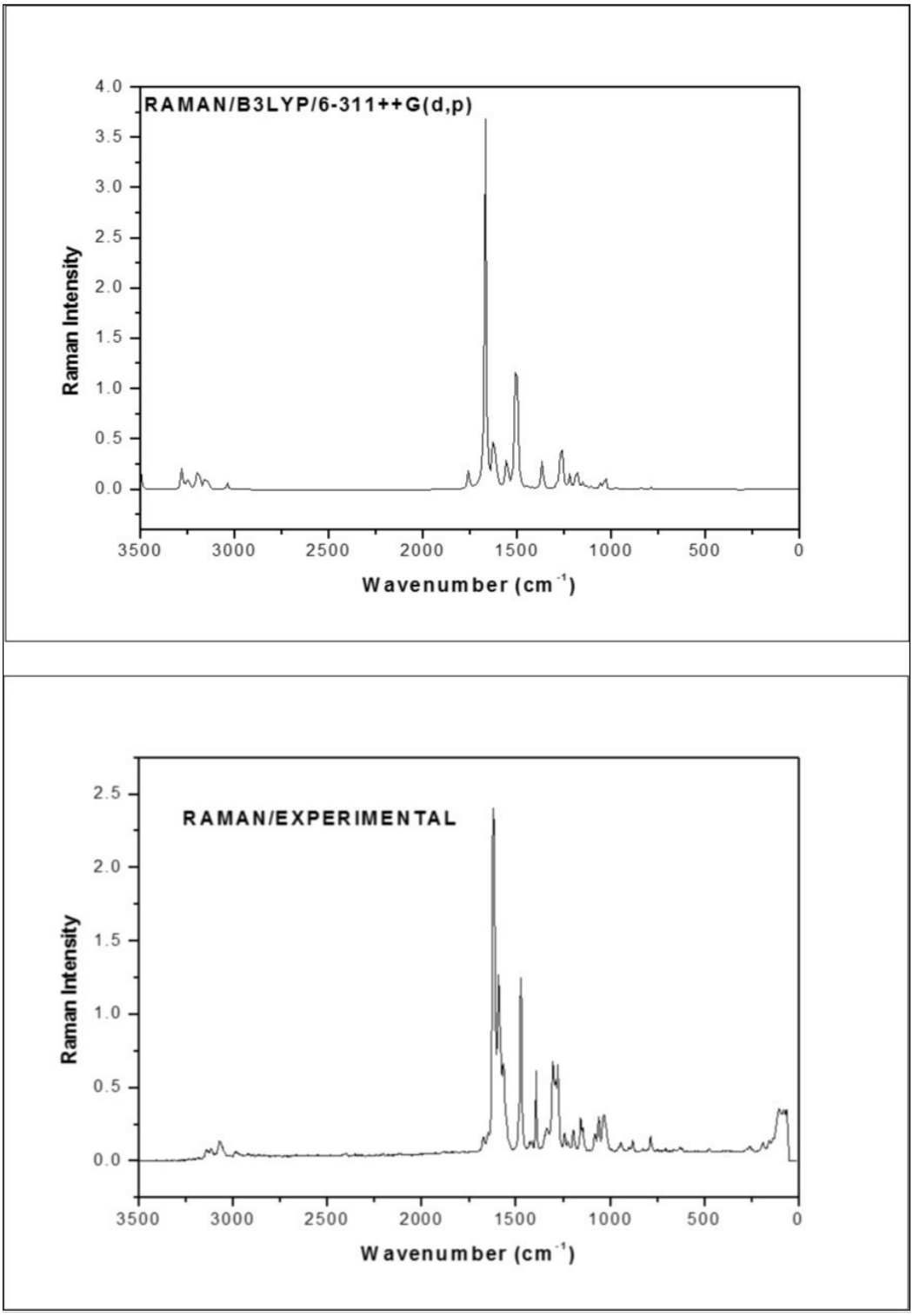

Figure 3. The Theoretical and Experimental FT-Raman spectra of F2CNH

belongs to Cs point group symmetry and has 25 atoms; hence 69 normal modes of vibrations are possible. The fundamental modes are distributed as: Γvib = 47A′ + 22A″. All vibrations are active in both IR and Raman absorption. The harmonic wavenumbers were calculated using DFT/B3LYP/6-311++G(d,p) basis set and are listed in Table 2. The vibrational assignments were made by visual inspection of modes animated by using the Gauss view [17] program and are also justified with the help of TED analysis. The combined vibrational spectra of F2CNH are shown in Figure 2 and Figure 3.

Table 2. The experimental and calculated frequencies of F2CNH using B3LYP/ 6-311++G(d,p) level of basis set harmonic frequencies (cm^{-1}) IR Raman intensities (Km/mol) reduced masses (amu) and force constants ($mdynA°^{-1}$)

Mode No	Calculated Frequencies (cm^{-1})	Observed Frequencies (cm^{-1})		IR Intensity	Raman Intensity	Vibrational Assignments≥10% (TED) [d]
	Scaled [a]	FT-IR	FT-Raman	Rel. [b]	Rel. [c]	
1	3367			2.01	1.55	$VN_{12}H_{13}(100)$
2	3151			0.07	1.09	$VC_5H_8(84)$
3	3135			0.24	0.22	$VC_3H_6(86)$
4	3119	3120 w	3117 w	1.07	0.74	$VC_4H_7(85)$
5	3076		3071 w	1.90	0.89	$VC_{17}H_{20}(90)$
6	3061	3069 m		2.58	1.04	$VC_{19}H_{24}(94)$
7	3032			3.04	0.88	$VC_{23}H_{25}(92)$
8	3016		2986 w	8.10	0.37	$VC_{18}H_{22}(98)$
9	2919	2926 w		10.18	0.45	$VC_9H_{10}(100)$
10	1689	1682 m	1673 w	100.00	5.15	$VO_{15}C_{14}(85)$
11	1604	1633 s	1621 s	6.67	100.00	$VN_{11}C_9(73)+\beta H_{10}C_9N_{11}(11)$
12	1563	1561 m	1568 m	8.77	14.37	$VC_{17}C_{19}(26)+\beta C_{17}C_{16}C_{18}(11)$
13	1553			17.15	8.42	$VC_4C_5(15)+VC_2C_3(42)+VC_9C_2(14)$
14	1542			1.53	0.51	$VN_{21}C_{23}(20)+VC_{23}C_{19}(24)+\beta C_{16}C_{18}N_{21}(16)+\beta C_{18}N_{21}C_{23}(13)$
15	1495		1475 s	99.44	12.34	$VN_{12}C_{14}(12)+\beta H_{13}N_{12}N_{11}(58)$
16	1449	1469 m		6.60	31.71	$VC_4C_5(22)+\beta H_{24}C_{19}C_{17}(15)+\beta H_{22}C_{18}C_{16}(15)$
17	1443	1428 m	1426 w	2.74	31.53	$VC_4C_5(43)+\beta H_8C_5O_1(31)$
18	1391		1394 m	7.33	0.73	$\beta C_{16}C_{18}N_{21}(22)+\beta H_{25}C_{23}N_{21}(42)$
19	1367			3.46	0.64	$VC_4C_3(22)+\beta H_7C_4C_5(18)+\beta H_8C_5O_1(13)+\beta H_{10}C_9N_{11}(10)$
20	1315	1337 s		12.87	10.80	$VC_4C_3(24)+\beta H_{10}C_9N_{11}(40)$
21	1308	1295 w	1304 m	1.38	0.86	$\beta H_{20}C_{17}C_{19}(29)+\beta H_{22}C_{18}C_{16}(39)$
22	1240		1244 w	5.38	1.75	$VC_{17}C_{19}(18)+VN_{21}C_{18}(48)$
23	1219			35.93	5.09	$VC_4C_3(11)+\beta H_6C_3C_4(24)+\beta H_8C_5O_1(13)$
24	1215	1214 m	1198 w	46.30	25.24	$\beta C_{17}C_{16}C_{18}(11)+VC_{16}C_{14}(17)+\beta H_6C_3C_4(10)$

 DOI: 10.14302/issn.2377-2549.jndc-16-949

Table 2 (continued)

Mode No	Calculated Frequencies (cm^{-1})	Observed Frequencies (cm^{-1})		IR Intensity	Raman Intensity	Vibrational Assignments≥10% (TED) [d]
	Scaled [a]	FT-IR	FT-Raman	Rel. [b]	Rel. [c]	
25	1174			13.24	6.89	$\nu N_{21}C_{23}(27)+\beta H_{24}C_{19}C_{17}(11)+\beta H_{25}C_{23}N_{21}(20)$
26	1170		1158 w	0.80	0.63	$\nu O_1C_2(31)+\beta H_{10}C_9N_{11}(15)$
27	1138	1153 m		21.11	14.35	$\nu O_1C_5(19)+\nu N_{12}N_{11}(21)+\beta H_8C_5O_1(20)$
x	1108			45.00	4.24	$\nu N_{12}C_{14}(12)+\nu N_{12}N_{11}(15)+\beta H_8C_5O_1(15)$
30	1067	1062 m	1062 w	13.11	1.64	$\nu C_4C_5(12)+\nu O_1C_5(43)$
31	1041		1035 w	4.01	0.58	$\nu N_{12}C_{14}(14)+\nu N_{12}N_{11}(23)$
32	1016	1020 m		0.37	3.90	$\nu N_{21}C_{23}(16)+\nu C_{23}C_{19}(36)$
33	999			4.05	2.29	$\beta C_{18}N_{21}C_{23}(24)+\beta C_{19}C_{23}N_{21}(18)+\beta C_{23}C_{19}C_{17}(36)$
34	993			6.44	7.61	$\nu C_4C_3(28)+\beta H_6C_3C_4(30)+\beta H_7C_4C_5(29)$
35	974			0.67	0.07	$\tau H_{20}C_{17}C_{19}H_{24}(77)+\tau H_{25}C_{23}N_{21}C_{18}(16)$
36	948		945 w	0.31	0.06	$\Gamma C_{17}C_{16}C_{19}H_{20}(31)+\Gamma C_{18}C_{16}C_{21}H_{22}(11)+\tau H_{25}C_{23}N_{21}C_{18}(47)$
37	938	938 w		5.90	1.77	$\nu C_2C_3(13)+\nu O_1C_2(27)+\beta C_2O_1C_5(20)$
38	910			3.58	0.52	$\tau H_{10}C_9N_{11}N_{12}(86)$
39	909			0.39	0.09	$\Gamma C_{18}C_{16}N_{21}H_{22}(72)$
40	881	878 w	882 w	4.65	0.32	$\beta N_{12}C_{14}O_{15}(40)+\beta C_{14}N_{12}N_{11}(11)+\beta C_2O_1C_5(17)$
41	867			5.71	0.63	$\beta C_4C_3C_2(45)+\beta C_2O_1C_5(34)$
42	859			0.05	0.23	$\tau H_6C_3C_4C_5(31)+\tau H_7C_4C_5H_8(53)+\tau H_8C_5C_4C_3(10)$
43	807	827 w		2.42	1.33	$\Gamma C_{17}C_{16}C_{19}H_{20}(34)+\tau H_{20}C_{17}C_{19}H_{20}(16)+\Gamma O_{15}C_{16}N_{12}C_{14}(13)+\Gamma C_{18}C_{16}N_{21}H_{22}(20)$
44	802		787 w	4.00	0.04	$\tau H_6C_3C_4C_5(55)+\tau H_7C_4C_5H_8(34)$
45	759	756 m		6.99	1.88	$\beta N_{11}C_9C_2(18)+\beta C_4C_3C_2(15)+\beta C_2O_1C_5(19)+\Gamma C_{14}C_{16}C_{18}C_{17}(20)$
46	720			19.50	0.41	$\tau H_7C_4C_5H_8(12)+\tau H_8C_5C_4C_3(75)$
47	710	705 w		6.96	0.70	$\Gamma C_{17}C_{16}C_{19}H_{20}(15)+\Gamma O_{15}C_{16}N_{12}C_{14}(45)$
48	696			5.95	0.36	$\beta C_{19}C_{23}N_{21}(19)+\tau C_{16}C_{23}C_{18}N_{21}(15)+\tau C_{19}C_{17}C_{23}N_{21}(11)$

 DOI: 10.14302/issn.2377-2549.jndc-16-949

Table 2 (continued)

Mode No	Calculated Frequencies (cm^{-1})	Observed Frequencies (cm^{-1})		IR Intensity	Raman Intensity	Vibrational Assignments≥10% (TED) [d]
	Scaled [a]	FT-IR	FT-Raman	Rel. [b]	Rel. [c]	
49	690			5.30	0.09	$\tau C_{16}C_{23}C_{18}N_{21}(27)+\tau C_{18}N_{21}C_{19}C_{23}(16)+\tau C_{19}C_{17}C_{23}N_{21}(21)$
50	640			0.02	0.08	$\tau C_3C_2C_4C_5(12)+\tau C_3C_5C_2O_1(66)$
51	609			1.10	0.60	$\beta C_{16}C_{18}N_{21}(20)+\beta C_{18}N_{21}C_{23}(32)+\beta C_{23}C_{19}C_{17}(28)$
52	581	582 w		2.36	0.10	$\tau C_3C_2C_4C_5(50)+\tau C_3C_5C_2O_1(26)$
53	523	521 w		2.31	1.21	$\beta C_{16}C_{18}N_{21}(24)+\Gamma H_{13}N_{12}N_{11}C_9(30)$
54	493			13.68	1.56	$\tau H_{13}N_{12}N_{11}C_9(80)$
55	466			0.35	1.05	$\beta C_{17}C_{16}C_{18}(12)+\beta N_{11}C_9C_2(11)+\beta C_9C_2O_1(18)$
56	405	419 w		2.43	0.12	$\tau C_{16}C_{23}C_{18}N_{21}(19)+\tau C_{18}N_{21}C_{19}C_{23}(32)$
57	383			0.83	0.13	$\tau C_{16}C_{23}C_{18}N_{21}(16)+\tau C_{19}C_{17}C_{23}N_{21}(32)$
58	370			0.37	0.09	$\beta C_{17}C_{16}C_{18}(15)+VC_{16}C_{14}(14)+\beta N_{12}C_{14}O_{15}(19)+\tau N_{12}N_{11}C_9C_2(11)$
59	348			0.42	0.43	$\tau N_{12}N_{11}C_9C_2(29)+\tau C_5O_1C_2C_9(14)$
60	258			3.81	0.42	$\beta C_{18}C_{16}C_{14}(32)$
61	238			0.14	1.01	$\beta C_9C_2O_1(20)+\beta C_{14}N_{12}N_{11}(21)$
63	167		191 w	3.13	1.44	$\beta C_{18}C_{16}C_{14}(10)+\tau C_3C_2C_9N_{11}(18)+\tau C_{14}N_{12}N_{11}C_9(24)+\Gamma C_{14}C_{16}C_{18}C_{17}(14)$
64	131			0.76	1.19	$\tau C_{14}N_{12}N_{11}C_9(15)+\tau N_{12}N_{11}C_9C_2(11)+\tau C_5O_1C_2C_9(41)$
65	118		107 w	2.15	0.78	$\beta N_{11}C_9C_2(19)+\beta C_9C_2O_1(14)+\beta C_{16}C_{14}N_{12}(18)+\Gamma C_{14}C_{16}C_{18}C_{17}(13)$
66	66			1.44	3.86	$\tau C_3C_2C_9N_{11}(16)+\tau C_{18}C_{16}C_{14}N_{12}(41)+\tau C_{14}N_{12}N_{11}C_9(13)+\tau C_5O_1C_2C_9(11)$
67	47			0.23	2.59	$\beta N_{11}C_9C_2(16)+\beta C_{14}N_{12}N_{11}(23)+\beta N_{12}N_{11}C_9(19)+\beta C_{16}C_{14}N_{12}(15)$

Table 2 (continued)

Mode No	Calculated Frequencies (cm^{-1})	Observed Frequencies (cm^{-1})		IR Intensity	Raman Intensity	Vibrational Assignments≥10% (TED) [d]
	Scaled [a]	FT-IR	FT-Raman	Rel. [b]	Rel. [c]	
68	35			0.05	4.48	$\tau C_3C_2C_9N_{11}(24)+\tau N_{12}N_{11}C_9C_2(23)+\tau C_{16}C_{14}N_{12}N_{11}(36)$
69	31			0.73	8.59	$\tau C_{18}C_{16}C_{14}N_{12}(41)+\tau C_{14}N_{12}N_{11}C_9(26)+\tau C_{16}C_{14}N_{12}N_{11}(14)$

n: Stretching, β: in-plane-bending, Γ: out-of-plane bending, τ- Torsion, vw: very weak, w:weak, m:medium, s:strong, vs:very strong,
[a] Scaling factor: 0.9608,
[b] Relative IR absorption intensities normalized with highest peak absorption equal to 100,
[c] Relative Raman intensities calculated by Equation (1) and normalized to 100.
[d] Total energy distribution calculated at B3LYP/6-311++G(d,p) level

C-H Vibrations

The heteroaromatic molecule shows the presence of C-H stretching mode in the region 3100-3000 cm^{-1} which is the characteristic region for the ready identification of C-H stretching [28], [29]. In this molecule, nine C-H stretching vibrations are expected to occur in which, four from pyridin ring, three from furan ring and one from hydrazone linkage. The pyridin ring C-H stretching vibrations observed at 3069 (m) in FT-IR whereas FT-Raman shown at 3071 and 2986cm^{-1} which is moderately in line with our earlier study [16]. The calculated wavenumbers for the same mode lie at 3076, 3061, 3032 and 3016 cm^{-1} (mode nos: 5-8). The experimental C-H stretching modes corresponding to furan ring are assigned to 3120 cm^{-1}/FT-IR and 3117 cm^{-1} in FT-Raman and their harmonic value lies at 3151, 3135 and 3119 cm^{-1} (mode nos: 2-4). The C-H stretching in hydrazone linkage is calculated at 2919 cm^{-1} and its corresponding experimental value at 2926 cm^{-1} in FTIR spectrum (mode no: 9) which is close to the value of literature [16]. Furthermore, these assignments are in good agreement with literature [28], [29], [30] and also find support from TED value [≥ 85%].

In aromatic compounds the C-H in-plane bending mode appears in the range 1300–1000 cm^{-1} and C-H out-of-plane bending mode appears in the range 1000-750 cm^{-1} [31], [32]. In the pyridine moiety of F2CNH, we observed the β_{CH} modes at 1469, 1295 cm^{-1} (FT-IR)/ 1304, 1081 cm^{-1} (FT-Raman) and Γ_{CH} modes at 825 (FT-Raman)/827, 705 cm^{-1} (FT-IR) and their corresponding calculated frequencies are in the range of 1449-1090 cm^{-1} (mode nos: 16, 21, 25, 29) and 948-710 cm^{-1} (mode nos: 36, 39, 43, 47), respectively. On comparing these observed values with calculated values, the mode numbers 21, 29 and 36, 43 are having ≥42% of TED value.

The bands between 1230 and 970 cm^{-1} in furan are assigned to β_{CH} modes [33]. The bands for the in-plane/ out-of-plane bending modes of CH in furan ring are identified at 1153/787 cm^{-1} in FTIR/ FT-Raman spectra. For the same mode the corresponding harmonic frequencies are: 1219, 1138, 993 cm^{-1} (mode nos: 23, 27, 34) and 859, 802, 720 cm^{-1} (mode nos: 42, 44, 46), respectively. These assignments are in good agreement with the assignments proposed by Subramanian et al., (2010) [34] and Balachandran et al., (2013) [33]. Further, the mode nos: 20 and 38 are attributed respectively to β_{CH} and Γ_{CH} modes of hydrazone linkage. These assignments are made in accordance with the assignments proposed by Ramesh Babu et al., (2014) [14] and also find support from observed FTIR band 1337 cm^{-1}. All the deformations (β_{CH} and Γ_{CH}) are having considerable TED values.

C=O, C-O Vibrations

The C=O stretching band is characterized by a sharp intense band appearing in between 1680 and 1715 cm^{-1} [35], [36]. According to this, the sharp intense bands in FTIR: 1682/FT-Raman: 1673 cm^{-1} spectra are assigned to $C_{14}=O_{15}$ stretching mode, whereas in our previous study [16] values shown at 1661/1663 in FT-IR/FT Raman respectively which is also confirmed by literature [14] and also find support from

harmonic value: 1689 cm^{-1} (mode no: 10). The $\beta C_{14}=O_{15}$ mode is assigned at 881 cm^{-1} (mode no: 40) in comparison with literature [14]. In our study, the bands observed at 878 and 882 cm^{-1} are due to $\beta_{C=O}$ mode in FTIR and FT-Raman spectra, respectively. The calculated TED (40%) corresponding to this mode shows that this mode is not a pure mode but contaminated with β_{CNN} and β_{COC} modes as shown in Table 2. The mode no: 47 (710 cm^{-1}) having TED value (45%) is attributed to $\Gamma_{C=O}$ mode, which is in agreement with the observed FTIR bands at 705 cm^{-1}. These C=O deformation vibrations are well supported by literature [14].

According to Ramesh Babu et al., (2014) [14], the harmonic frequencies of C-O stretching in furan ring appear in the range 1193-905 cm^{-1}. The frequency of the νO_1-C_5 and νO_1-C_2 vibrations are calculated to be 1170 and 1067 cm^{-1}, respectively for F2CNH and these modes are observed in the FT-Raman spectrum at 1158 and 1062 cm^{-1} (FTIR: 1062 cm^{-1}) with weak intensity. These assignments are well within the expected range and they have considerable TED values (31% and 43%). The β_{COC} (mode nos: 37, 45) and τ_{COC} (mode nos: 59, 64) vibrations are presented in Table 2. These assignments are also supported by the literature [33] in addition to TED output.

C=N, C-N and N-N Vibrations

The IR and Raman bands observed between 1443 and 1227 cm^{-1} in pyridine derivatives have been assigned to ν_{C-N} vibrations [37]. In general, a pure mode cannot be expected for ν_{C-N} vibrations since it falls in a complicated region of the vibrational spectrum. In F2CNH the C_{18}-N_{21}/C_{23}-N_{21} stretching vibrations assigned at 1240/1542 cm^{-1} (mode nos: 22, 14) as mixed vibrations of $\nu_{CC}+\beta_{CCN}/\beta_{CCC}+\beta_{HCN}$ modes respectively. In which mode no: 22 correlates well with observed FT-Raman value 1244 cm^{-1} and also finds support from TED value 48%.

In this work, the hydrazone linkage fuses the pyridine and furan rings, which leads the vibrations such as $\nu_{C=N}$, ν_{C-N} and ν_{N-N} modes. According to Socrates (1980) [31] the frequencies of $\nu_{C=N}$ appear around 1600-1670 cm^{-1}. In our earlier study, the $\nu_{C=N}$ vibration assigned at 1611: FTIR/1627 cm^{-1}: FT-Raman [14]. In our earlier investigation [16], FT-Raman shown at 1606 and Rameshbabu et, al., [14] assigned $\nu_{C=N}$, vibration at 1611:FTIR / 1627:FT-Raman. Based on this literature, the scaled harmonic wavenumber of $\nu C_9=N_{11}$ mode depicted in Table 2 (1604 cm^{-1}/mode no: 11) is found to be in agreement with experimental data: 1633 cm^{-1} in FTIR as well as in FT-Raman spectra (1621 cm^{-1}). Silverstein et al., (1981) [29] assigned C-N stretching absorption in the region 1382-1266 cm^{-1} for aromatic amines. In the present study, the band observed at 1475 cm^{-1} in FT-Raman spectrum which is exactly matches with our earlier study [14] at 1606/FT-Raman and its corresponding calculated value 1495 cm^{-1} (mode no: 15) are assigned to νC_{14}-N_{12} mode. The same mode was recorded at 1516 cm^{-1} (FTIR) by Rameshbabu et. Al., [14]. The ν_{N-N} mode was observed as a medium intense band at 1128 cm^{-1} /FTIR and at 1137 cm^{-1}/FT-Raman [22]. The νN_{11}-N_{12} vibration is observed as a medium intense band in FTIR at 1153 cm^{-1} (Harmonic/mode no: 27/1138 cm^{-1}) has 21% of this stretching character because of its association with ν_{CO} and β_{HCO} vibrations and this assignment is further supported by literature [14].

The βC_2-$C_9=N_{11}/\Gamma C_2$-$C_9=N_{11}$ vibrations are assigned at 756 (FTIR)/348 cm^{-1} (harmonic) and that of βC_{14}-N_{12}-$N_{11}/\Gamma C_{14}$-C_{12}-N_{11} are assigned at 878 (FTIR)/191 cm^{-1} (FTIR) respectively, in comparison with their corresponding harmonic values (mode nos: 45/59 and 40/63). The theoretically computed values for $\beta C_9=N_{11}$-N_{12} and $\Gamma C_9=N_{11}$-N_{12} vibrations come out to be 47 cm^{-1} (mode no: 67) and 31 cm^{-1} (mode no: 69) respectively. These assignments are having considerable TED values.

N-H Vibrations

The N-H stretching vibrations occur in the region 3400-3200 cm^{-1} [38] and Ramesh babu et. al., [14] observed at 3246 cm^{-1} in FTIR spectrum. In agreement with these observation, in the present case also this band at 3367 cm^{-1} (mode no: 1) is assigned to stretching frequency of N-H group. This assignment is straight forward on the basis of their calculated TED value (100 %). The calculated wavenumber for β_{N-H} (1495 cm^{-1}/mode no: 15) and Γ_{N-H} (523 cm^{-1}/ mode no: 53) modes well reproduced the experimental ones in FT-Raman (1475 cm^{-1}) and FTIR (521 cm^{-1}) spectra, respectively. These assignments are made in accordance with the literature [14] and also find support from their respective TED values (58% and 30%).

C=C, C-C Vibrations

In furan derivatives, medium to strong bands have appeared in the regions of 1390-1400, 1470-1520, 1560-1610 cm^{-1}, which are due to the C=C ring stretching vibrations [27]. In general, furan with electronegative substituent has strong bands in these regions. Usually Five membered ring compounds with two doublet bond in ring, shows three ring stretching bands near 1400, 1490 and 1590 cm^{-1} [39].

In our present study, the C=C stretching bands observed at 1469 (m), 1428 (m), and 1337 cm^{-1} (s) in FT-IR spectrum, whereas FT-Raman band observed at 1426 as weak band. On the other hand, $\nu_{c=c}$ bands were predicted at 1449, 1443 and 1315 cm^{-1} (mode nos: 16, 17 and 20) and in good agreement with literature [14]. The mode nos: 41, 45 and 50, 52 belong to β_{CCC} and Γ_{CCC} modes, respectively. In which mode nos: 45 (759 cm^{-1}) and 52 (581 cm^{-1}) are justified by the observed FTIR bands at 756 and 582 cm^{-1} and also find support from TED value.

The C-C stretching was assigned in the region 1668-1218 cm^{-1} for some substituted pyridines [37]. Ramesh Babu et al., [40] assigned 1532 (w), 1370, 1261 cm^{-1} in FT-Raman and 1361, 1266 cm^{-1} (w) in FTIR spectra are assigned to $\nu_{(C-C)}$ vibrations of pyridine ring in the case of *(E)-N'-((pyridine-2-yl)methylene)benzohydrazide*. In view of the above, the harmonic frequencies in the range 1563-1016 cm^{-1} (mode nos: 12, 22, 29, 32) and the bands observed at 1561, 1020/1568, 1244, 1081 cm^{-1} in FTIR/FT-Raman spectra are assigned to ν_{C-C} mode. These assignments are also supported by TED value.

The β_{CCC} and Γ_{CCC} modes associated with smaller force constant than the stretching one and hence assigned to lower frequencies. The harmonic frequencies 999, 609 and 405, 383 cm^{-1} (mode nos: 33, 51 and 56, 57) are assigned to β_{CCC} and Γ_{CCC} modes of pyridine ring. These assignments find support from literature [40] in addition to TED output. Further, the mode no: 56 is further supported by observed band (FTIR/419 cm^{-1}). The mode nos: 13 and 24 belong to νC_9-C_2 and νC_{16}-C_{14} modes.

NLO Property

The molecular electronic dipole moment and molecular first hyperpolarizability of F2CNH were calculated using B3LYP level and the obtained results were given in Table 3. The dipole moment was calculated as 0.9722 Debye which is comparatively closer to standard urea. The first order hyperpolarizability (β_0) was calculated as $2.0918x10^{-30}$ esu, which is six times greater than that of the value of the urea. Hence this molecule has considerable NLO activity.

NBO Analysis

The NBO analysis has been carried out with B3LYP/6-311++G(d,p) level of basis set. The Lewis and non-Lewis NBO's of the F2CNH are given in Table 4. The strong intra-molecular hyperconjugative interaction of the π and σ electrons of C-C to the anti C-C bond of the rings leads to stabilization of some part of the rings. The intra-molecular hyperconjugative interaction of $\pi(C_2-C_3)\rightarrow\pi^*(C_9-N_{11})$, $\pi(C_9-N_{11})\rightarrow\pi^*(C_2-C_3)$ and $\pi(N_{21}-C_{23})\rightarrow\pi^*(C_{16}-C_{18})$ leading to stabilization of 75.48, 41.17 and 113.09 KJ/mol, respectively. On the other hand the $\sigma(C_2-C_3)\rightarrow\sigma^*(C_2-C_9)$, $\sigma(C_9-N_{11})\rightarrow\sigma^*(N_{12}-C_{14})$ and $\sigma(C_{17}-C_{19})\rightarrow\sigma^*(C_{16}-C_{17})$ transition stabilize lesser energy 17.87, 9.46 and 12.01 KJ/mol, respectively. In such a way that the molecule F2CNH delivers maximum delocalization energy during π-π* transition whereas the electron density of the donor (Lewis) bond decreases with increasing of electron density of acceptor (Non-Lewis) bonds. The maximum energy transfer during the intra-molecular interaction between (π-π*) ($C_{17}-C_{19}$) and ($N_{21}-C_{23}$) is about 122.13 KJ/mol. This may be due to the hyperconjugative interaction between $C_{17}-C_{19}$ donor and $C_{23}-N_{21}$ acceptor bonds. It is evident from Table 4, the $\pi(C_{17}-C_{19})$ hyperconjugative interactions transfer more energy (122.13 KJ/mol) to the acceptor bond $\pi^*(N_{21}-C_{23})$ in pyridine ring. Hence the strong delocalization in pyridine is mainly due to the presence of C=N-C. Based on the fact, that the $\nu(C_{23}-N_{21})$ modes appear at higher frequency (1542 cm^{-1}) on comparing with $\nu(C_{18}-N_{21}$/1240 cm^{-1} mode. In F2CNH, the π-π* interaction appears with maximum delocalization energy which leads the molecule become highly active. The lone pair of oxygen and nitrogen atoms play greater role in the molecule F2CNH: $LPO_1\rightarrow C_4-C_5$ (114.47), $LPO_{15}\rightarrow N_{12}-C_{14}$ (118.41) and $LPN_{12}\rightarrow C_{14}-O_{15}$ (190.62 KJ/mol), respectively. These charge transfer interactions of F2CNH are responsible for more stabilization, medicinal and biological properties.

Table 3. The NLO measurements of F2CNH

Parameters	B3LYP/6-311++G(d,p)
Dipole moment (μ) **Debye**	
μ_x	-0.3453
μ_y	-0.7229
μ_z	0.5508
μ	0.9722**Debye**
Polarizability ($\boldsymbol{\alpha_0}$) x10^{-30}esu	
α_{xx}	313.9112
α_{xy}	0.06
α_{yy}	-0.0037
α_{xz}	0.0048
α_{yz}	-0.0112
α_{zz}	0.1032
$\boldsymbol{\alpha_o}$	0.6277**x10^{-30}esu**
Hyperpolarizability ($\boldsymbol{\beta_0}$)**x**10^{-30}esu	
β_{xxx}	2472.1702
β_{xxy}	254.6161
β_{xyy}	15.47
β_{yyy}	-93.8977
β_{xxz}	30.3521
β_{xyz}	-22.69
β_{yyz}	12.4543
β_{xzz}	-72.4323
β_{yzz}	-0.8853
β_{zzz}	19.7437
β_0	2.0918**x10^{-30}esu**

Standard value for urea (**μ**=1.3732 Debye, $\boldsymbol{\beta_0}$=0.3728x10^{-30}esu): **esu**-electrostatic unit

Table 4. The second order perturbation theory analysis of Fock Matrix in NBO basis for F2CNH

Type	Donor NBO (i)	ED/e	Acceptor NBO (j)	ED/e	$E^{(2)}$ KJ/mol	E(j)-E(i) a.u.	F(i,j) a.u.
σ -σ*	BD (1) C_2 - C_3	1.98	BD*(1) C_2 - C_9	0.028	17.87	1.21	0.06
			BD*(1) C_3 - C_4	0.009	7.61	1.25	0.04
			BD*(1) C_3 - H_6	0.011	5.44	1.18	0.04
			BD*(1) C_4 - H_7	0.011	15.56	1.17	0.06
			BD*(1) C_9 - H_{10}	0.035	4.85	1.09	0.03
π -π*	BD (2) C_2 - C_3	1.792	BD*(2) C_4 - C_5	0.268	70.42	0.29	0.06
			BD*(2) C_9 - N_{11}	0.214	75.48	0.27	0.06
σ -σ*	BD (1) C_9 - N_{11}	1.986	BD*(1) N_{12} - C_{14}	0.085	9.46	1.33	0.05
			BD*(1) C_2 - C_9	0.028	7.82	1.39	0.05
π -π*	BD (2) C_9 - N_{11}	1.925	BD*(2) C_2 - C_3	0.315	41.17	0.37	0.06
σ -σ*	BD (1) C_{17} - C_{19}	1.979	BD*(1) C_{16} - C_{17}	0.021	12.01	1.27	0.05
π -π*	BD (2) C_{17} - C_{19}	1.636	BD*(2) C_{16} - C_{18}	0.336	74.81	0.28	0.06
			BD*(2) N_{21} - C_{23}	0.366	122.13	0.27	0.08
π -π*	BD (2) N_{21} - C_{23}	1.706	BD*(2) C_{16} - C_{18}	0.336	113.09	0.32	0.08
			BD*(2) C_{17} - C_{19}	0.277	52.59	0.32	0.06
n -π*	LP (2) O_1	1.708	BD*(2) C_2 - C_3	0.315	108.78	0.37	0.09
			BD*(2) C_4 - C_5	0.268	114.47	0.36	0.09
n -π*	LP (2) N_{12}	1.666	BD*(2) C_9 - N_{11}	0.214	117.24	0.28	0.08
			BD*(2) C_{14} - O_{15}	0.277	190.62	0.32	0.11
n -π*	LP (2) O_{15}	1.855	BD*(2) N_{12} - C_{14}	0.085	118.41	0.67	0.12
			BD*(2) C_{14} - C_{16}	0.069	80.33	0.66	0.1
n -σ*	LP (1) N_{21}	1.916	BD*(1) C_{16} - C_{18}	0.033	39.33	0.9	0.08
			BD*(1) C_{18} - H_{22}	0.025	17.32	0.76	0.05
			BD*(1) C_{19} - C_{23}	0.026	37.45	0.9	0.08
			BD*(1) C_{23} - H_{25}	0.023	16.99	0.77	0.05
π*-π*	BD*(2) C_9 - N_{11}	0.214	BD*(2) C_2 - C_3	0.315	330.75	0.02	0.08
π*-σ*	BD*(2) C_{14} - O_{15}	0.277	BD*(1) C_{14} - O_{15}	0.017	12.59	0.56	0.1
π*-π*	BD*(2) C_{16} - C_{18}	0.336	BD*(2) C_{14} - O_{15}	0.277	369.99	0.02	0.07
π*-π*	BD*(2) N_{21} - C_{23}	0.366	BD*(2) C_{16} - C_{18}	0.336	839.56	0.01	0.08
			BD*(2) C_{17} - C_{19}	0.277	590.7	0.02	0.08

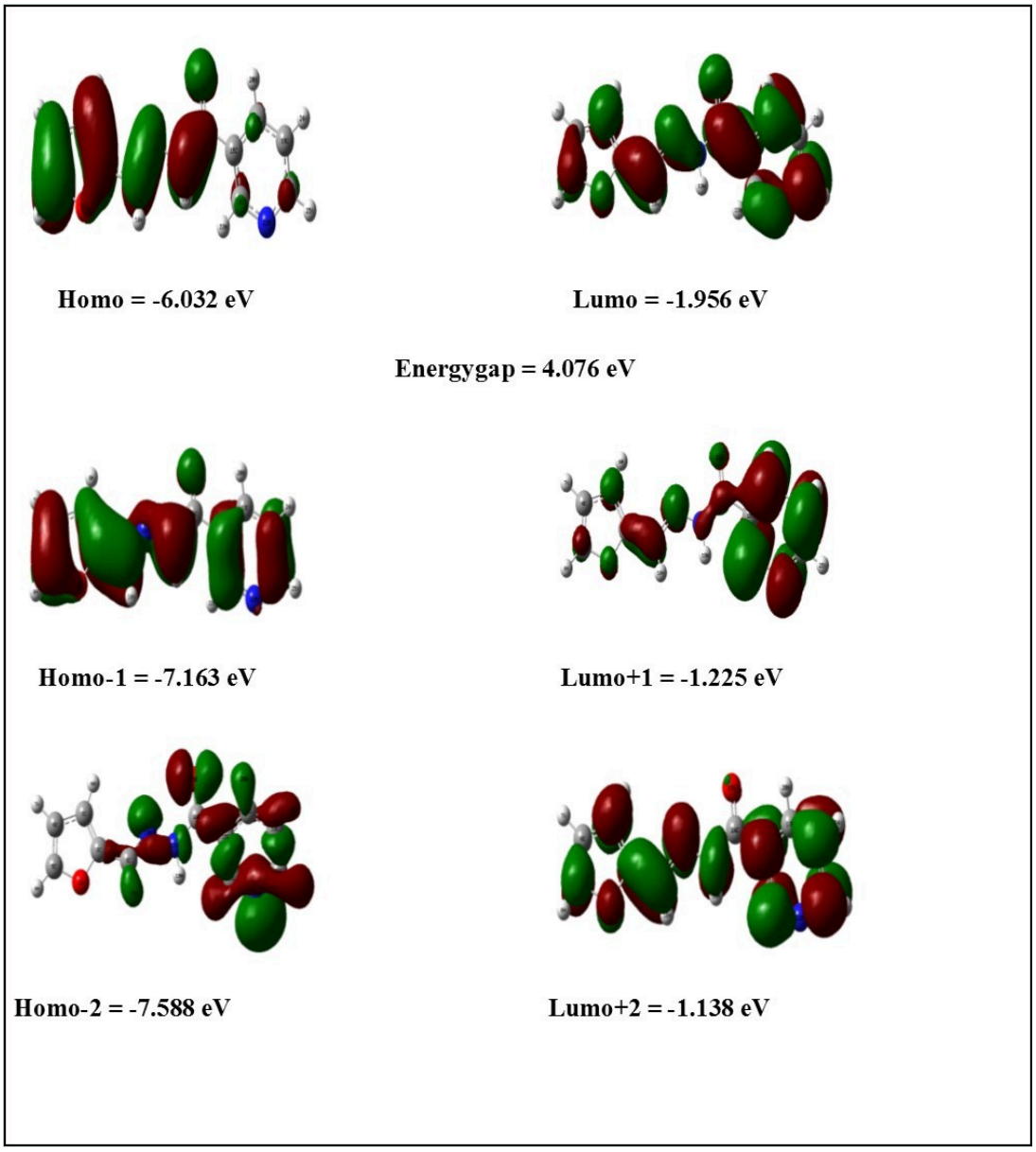

Figure 4. The frontier molecular orbital for F2CNH

HOMO-LUMO Analysis

The HOMO and LUMO are the main orbitals that take part in chemical stability. The HOMO represents the ability to donate an electron, whereas the LUMO is an electron acceptor which represents the ability to obtain an electron. This also predicted that the nature of electrophiles and nucleophiles to an atom where the HOMO and LUMO are stronger. The energy gap of F2CNH was calculated using B3LYP/6-311++G(d,p) level and is listed in Table 5. In the present study, the HOMO part is located over the furan ring and hydrazone linkage and HOMO energy is calculated about -6.032 eV. Similarly, the LUMO is located over the entire molecule and especially on pyridine ring and LUMO energy is -1.956 eV. The energy gap between HOMO and LUMO is 4.076 eV, which leads the molecule to become less stable and more reactive. The calculated energies of frontier molecular orbitals are listed in Table 6 and the frontier molecular orbitals are shown in Figure 4. The various frontier molecule orbitals of F2CNH and listed their corresponding orbital energies are in Table 6.

UV–Vis Spectra Analysis

The nature of the electronic transitions in the observed UV-visible spectrum of the title compound F2CNH had been studied by the TD-DFT involving configuration interaction between the singly existed

Table 5. The Physico-chemical properties of F2CNH

Parameters	Values
HOMO	-6.032 eV
LUMO	-1.956 eV
Energy gap	4.076 eV
Ionization potential (IP)	6.032 eV
Electron affinity (EA)	1.956 eV
Electrophilicity Index (ω)	2.562
Chemical Potential (μ)	3.994
Electro negativity (χ)	-3.994
Hardness (η)	-4.076

electronic states. The observed UV-vis spectrum was shown in Figure 5. The electronic transitions and the corresponding excitation energies were listed in Table 7. The calculated electronic transition is shown at 333 nm whereas the experimental electronic transition was observed at 360 nm. The difference in these two values may possibly be owing to solvent influence.

MEP Analysis

The molecular electrostatic potential (MEP) map was calculated using B3LYP/6-311++G(d,p) level of basis set. The 3D plot of MEP map of F2CNH is shown in Figure 6. In MEP map, the maximum positive/negative regions are preferred sites for nucleophilic/electrophilic attack and are represented by Blue/Red colour, respectively. The importance of MEP lies in the fact that it simultaneously displays molecular size, shape as well as positive, negative and neutral electrostatic potential regions in terms of color grading Figure 6 and is very useful in research of molecular structure with its physiochemical property relationship [41], [42].

Table 6. The frontier molecular orbital of F2CNH

Occupancy	Orbital energies a.u	Orbital energies eV	Kinetic energies a.u
O_{52}	-0.289	-7.875	1.618
O_{53}	-0.286	-7.792	1.516
O_{54}	-0.278	-7.588	1.735
O_{55}	-0.263	-7.163	2.213
O_{56}	-0.221	-6.032	1.591
V_{57}	-0.071	-1.956	1.666
V_{58}	-0.045	-1.225	1.639
V_{59}	-0.041	-1.138	1.582
V_{60}	0.022	6.035	1.581
V_{61}	0.025	0.696	0.94

DOI: 10.14302/issn.2377-2549.jndc-16-949

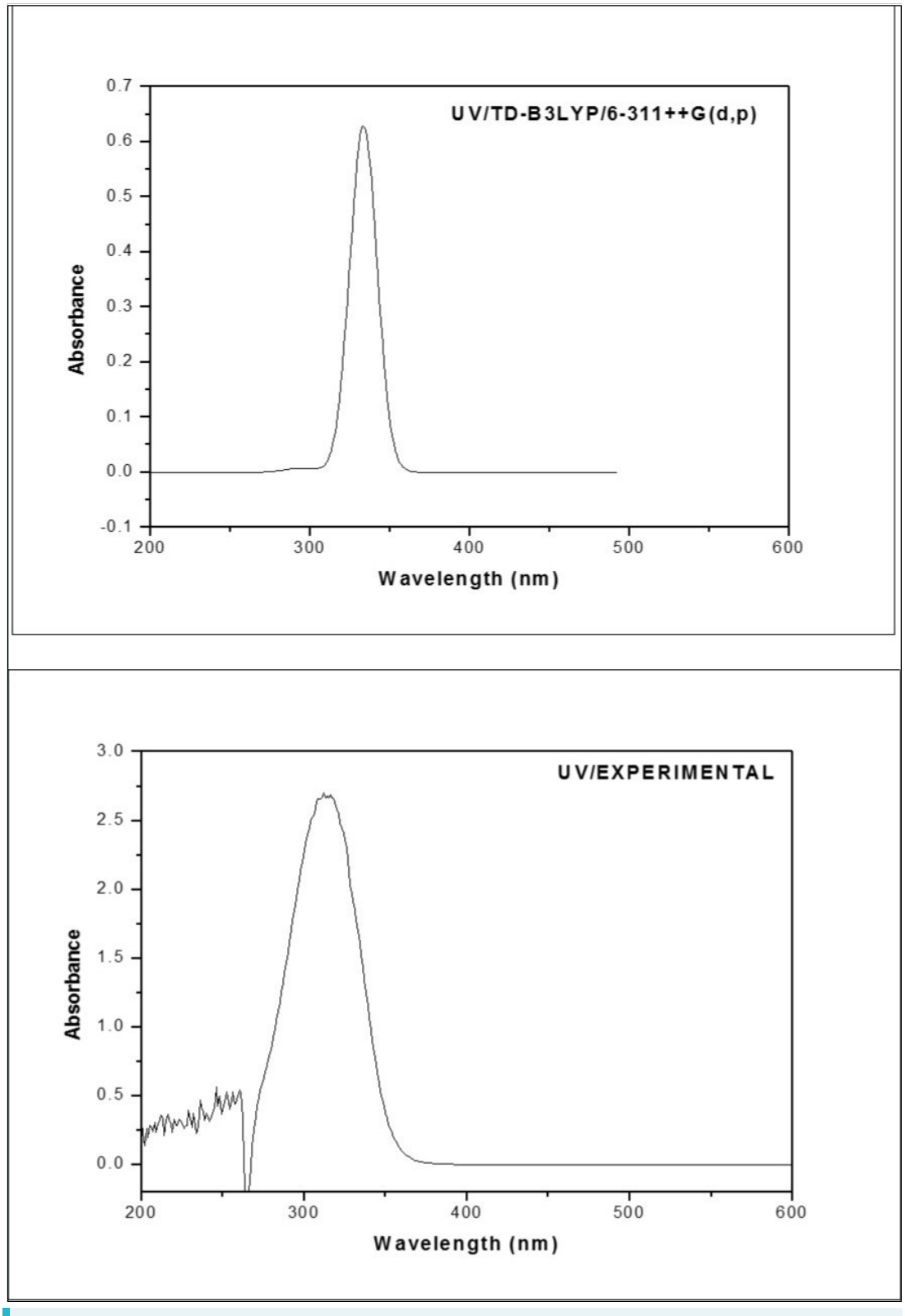

Figure 5. The Theoretical and Experimental UV-Visible spectra of F2CNH

The Potential increases in the order of red < orange < yellow < green < blue. The color code of this map is in the range between -6.471 a.u. (deepest red) to 6.471 a.u. (deepest blue) in F2CNH, where blue indicates the strongest attraction and red indicates the strongest repulsion. It can be seen from the MEP map of the F2CNH, the regions having the negative potential are over the carbonyl group while the regions having the positive potential are over all the hydrogen atoms.

Table 7. The electronic transition of F2CNH

Calculated at B3LYP/ 6-311++G(d,p)	Oscillator strength	Calculated Band gap (ev/nm)	Experimental Band gap (nm)	Type
Excited State 1	Singlet-A (f=0.6299)	3.7193 eV/333.35 nm	360 nm	π-π*
56 -> 57	0.6436	4.0763		
56 -> 58	0.1052	4.8069		
Excited State 2	Singlet-A (f=0.0039)	4.1291 eV/300.27 nm		
55 -> 57	0.658	5.2074		
55 -> 59	-0.1462	6.0253		
Excited State 3	Singlet-A (f=0.0047)	4.2664 eV/290.61 nm		
56 -> 58	0.5608	4.8069		
56 -> 59	0.4178	4.8942		

Mulliken Charge Analysis

Mulliken atomic charge calculation has an important role in the application of quantum chemical calculation to molecular system, since atomic charges affect the dipole moment, molecular polarizability, electronic structure and more a lot of properties of molecular systems. The Mulliken charges were calculated by DFT/B3LYP/6-311++G(d,p) basis set. The calculated Mulliken charge values are listed in Table 8 and are plotted in Figure 7. The carbonyl group has the most positive C_{14}: 0.440 and most negative charge O_{15}: -0.3255 and all the hydrogen atoms have positive charge.

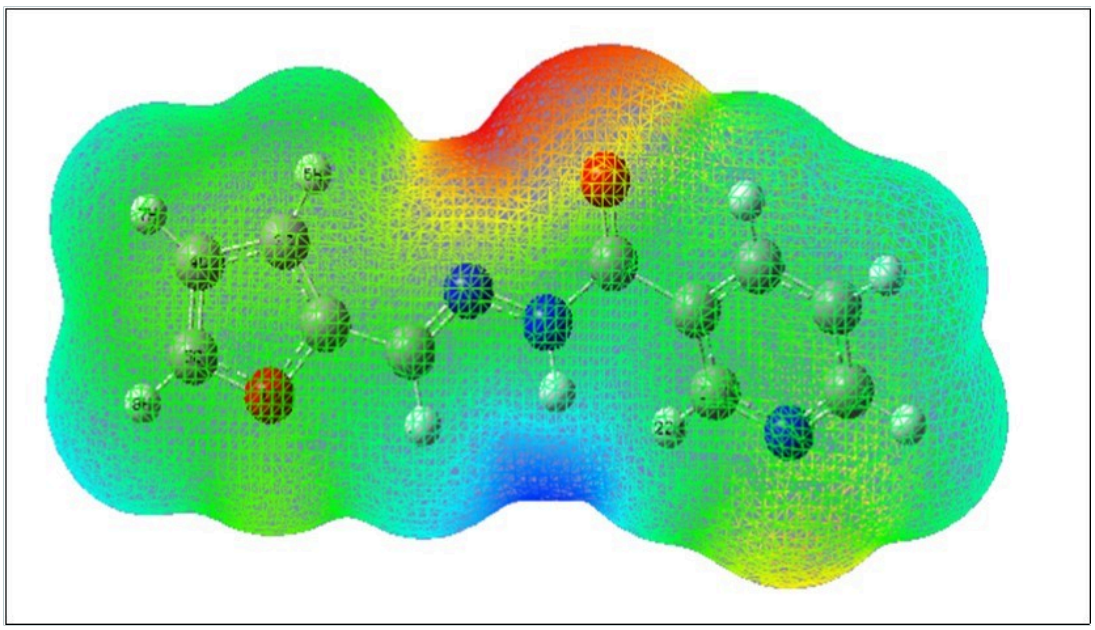

Figure 6. The Molecular electrostatic potential map of F2CNH

DOI: 10.14302/issn.2377-2549.jndc-16-949

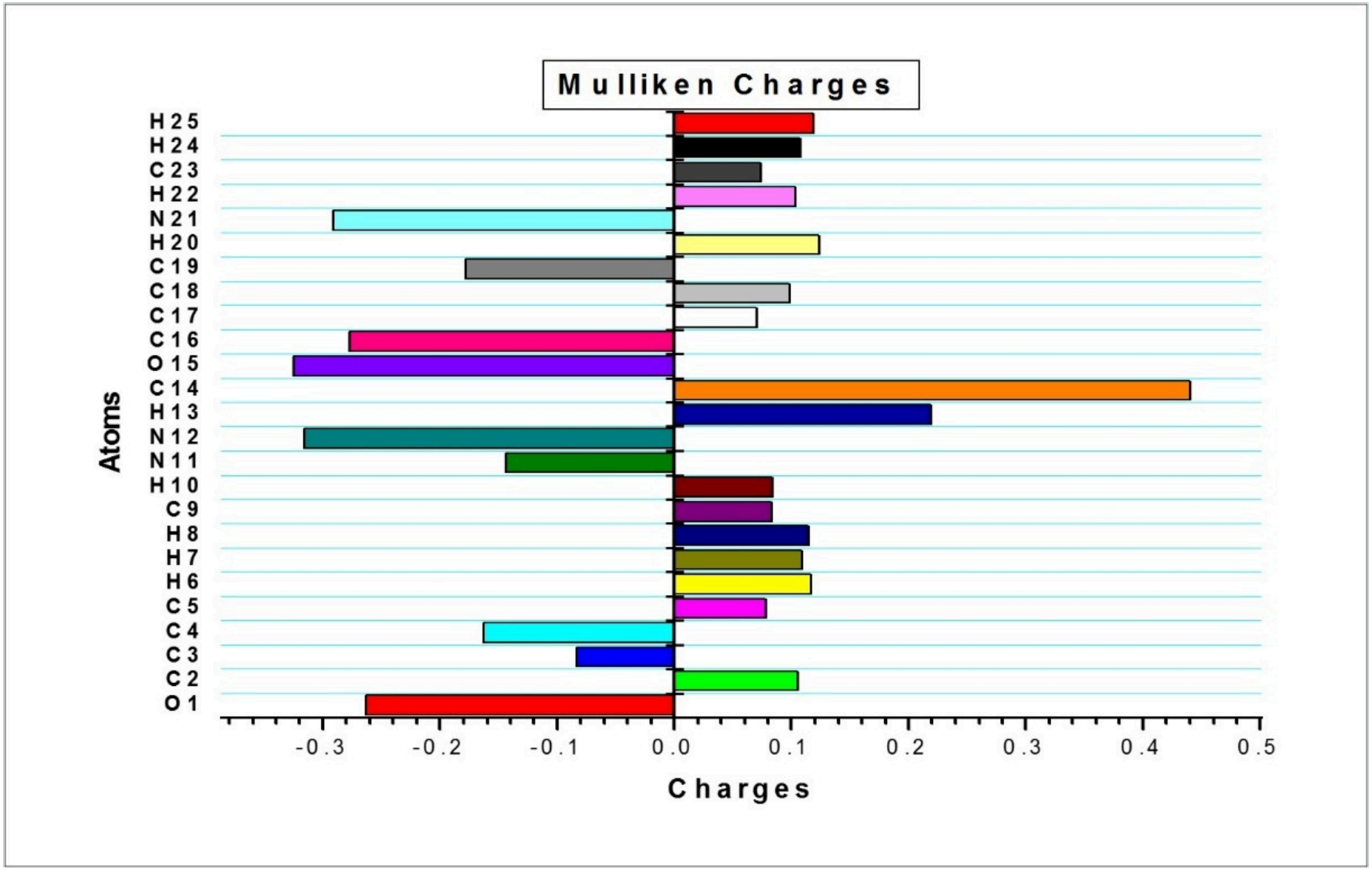

Figure 7. The Mulliken atomic charges of F2CNH

OPEN ACCESS

Table 8. The Mulliken atomic charges of F2CNH

Atoms	Charges	Atoms	Charges	Atoms	Charges
O_1	-0.263	H_{10}	0.0832	C_{19}	-0.1788
C_2	0.1051	N_{11}	-0.1439	H_{20}	0.1235
C_3	-0.0835	N_{12}	-0.3159	N_{21}	-0.291
C_4	-0.1635	H_{13}	0.2189	H_{22}	0.1033
C_5	0.0781	C_{14}	0.4399	C_{23}	0.0732
H_6	0.1163	O_{15}	-0.3255	H_{24}	0.1075
H_7	0.1089	C_{16}	-0.2773	H_{25}	0.1189
H_8	0.1145	C_{17}	0.0703		
C_9	0.0824	C_{18}	0.0979		

Thermodynamic Properties

The various thermodynamic parameters such as: total energies, zero-point energy etc were calculated using B3LYP/6-311++G(d,p) basis set and are presented in Table 9. On the basis of vibrational analysis, the statistical thermodynamic functions heat capacity ($C^0_{p,m}$), entropy (S^0_m), and enthalpy changes (ΔH^0_m) for the F2CNH were obtained from the theoretical harmonic frequencies listed in Table 10. It can be seen from Table 10, the thermodynamic functions are increasing with temperature ranging from 100 to 1000 K due to the fact that the molecular vibrational intensities increase with temperature. The correlation equations between heat capacity, entropy, enthalpy changes and temperatures were fitted by quadratic formulas and the corresponding fitting factors (R^2) for these thermodynamic properties are

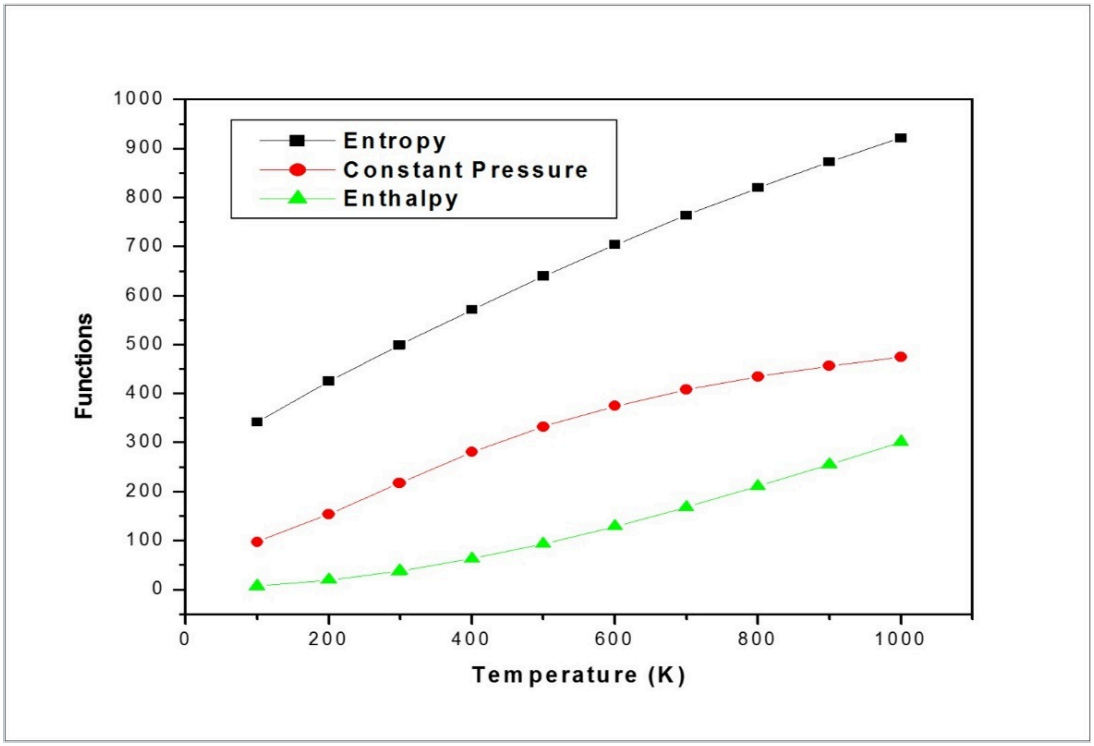

Figure 8. The thermodynamic properties at different temperatures of F2CNH

Table 9. The calculated total energy (a.u), zero point vibrational energies (Kcal/mol), rotational constants (GHz) and entropy (cal/mol K^{-1}) for F2CNH

Parameters	B3LYP/6-311++G(d,p)
Total Energies	-739.434
Zero-point Energy	117.048 (Kcal/Mol)
Rotational constants (GHZ)	2.117
	0.177
	0.165
Entropy	
Total	119.061
Translational	42.001
Rotational	32.915
Vibrational	44.145

0.99895, 0.99997 and 0.99946 respectively. The comparative thermodynamical graphs of F2CNH are shown in Figure 8. The corresponding fitting equations are as follows:

$C^0_{p,m} = 5.42703 + 0.02291T + 2.0243x10^{-5} T^2$ ($R^2 = 0.99895$)

$S^0_m = 1.24898 + 0.00527T + 4.65873x10^{-5} T^2$ ($R^2 = 0.99997$)

$\Delta H^0_m = 3.05729 + 0.01291T + 1.14038x10^{-5} T^2$ ($R^2 = 0.99946$)

All the given thermodynamic data are the helpful information for further study on F2CNH. They can be used to compute the other thermodynamic energies according to relationships of thermodynamic functions and estimate directions of chemical reactions according to the second law of thermodynamics

Table 10. Thermodynamic Properties at different temperatures of F2CNH

T (K)	S (J/mol.K)	Cp (J/mol.K)	ddH (kJ/mol)
100	341.24	97.36	6.77
200	425.36	153.35	19.22
298.15	498.26	216.68	37.35
300	499.6	217.89	37.75
400	570.98	279.98	62.71
500	639.27	332.23	93.41
600	703.68	374.06	128.81
700	763.94	407.38	167.94
800	820.16	434.28	210.07
900	872.62	456.34	254.64
1000	921.68	474.68	301.21

in thermochemical field [43]. All the thermodynamic calculations were done in gas phase and they could not be used in solution.

Conclusion

A complete vibrational analysis has been carried out for the first time to the molecule F2CNH. The optimized bond parameters agree well with the literature values. The observed FT-IR, FT-Raman and UV-Vis absorption spectral values are in good agreement with the calculated values. The first order hyperpolarizability (β_0=2.0918x10^{-30} esu) of F2CNH was calculated and found to be six times greater than that of urea and hence the molecule has considerable NLO activity. The hyperconjucative interaction $\pi(C_{17}\text{-}C_{19})\rightarrow\pi^*(N_{21}\text{-}C_{23})$ transfer more energy 122.13 kJ/mol, which leads the $\nu(C_{23}\text{-}N_{21})$ mode to appear at higher frequency (1542 cm^{-1}) than the $\nu(C_{18}\text{-}N_{21})$ mode. The Homo-Lumo energy gap was calculated about 4.076 eV. The UV-Vis study reveals that an electronic transition takes place from furan to pyridine ring via hydrazone linkage and is represented as π-π^* type. MEP surface analysis mentioned the active charge sites of the molecule F2CNH. In addition Mulliken charges and thermodynamic properties are also reported.

Competing Interests

The authors have declared that no competing interests exist.

References

1. Brown R C D. Developments in Furan Syntheses. *Ange. Chem. Int. Edn*. 2005;44:850–852. https://doi.org/10.1002/anie.200461668
2. Paquette LA, Astles PC. Total synthesis of furanocembranolides. 3. A concise convergent route to acerosolide. *J. Org. Chem*. 1993;58:165–169. https://doi.org/10.1021/jo00053a031
3. Forster H, Fuess H, Geidel E, Hunger B, Jobic H, Kirschhock C, Klepel O, Krause K. Adsorption of pyrrole derivatives in alkali metal cation-exchanged faujasites: comparative studies by surface vibrational techniques, X-ray diffraction and temperature-programmed desorption augmented with theoretical studies Part I. Pyrrole as probe molecule. *Phys. Chem. Chem. Phys*. 1999;1:593–603.
4. Beta IA, Bohlig H, Dobler J, Jobic H, Geidel E, Hunger B. Adsorption of furan, 2,5-dihydrofuran and tetrahydrofuran on sodium-ion exchanged faujasites with different Si/Al ratios. *Studies in Surface Science and Catalysis*. 2001;218.
5. Moro S, Chipman JK, Wegener JW, Hamberger C, Dekant W, Mally A. Furan in heat-treated foods: Formation, exposure, toxicity, and aspects of risk assessment. *Mol. Nutri. and food research*. 2012;56:1197–1211. https://doi.org/10.1002/mnfr.201200093
6. Anese M, Manzocco L, Calligaris S, Nicoli MC. Industrially Applicable Strategies for Mitigating Acrylamide, Furan and 5-Hydroxymethylfurfural in Food. *J. agri. food chem*. 2013. https://doi.org/10.1021/jf305085r
7. European Food Safety Authority. *EFSA Journal*. 2011;9(9):2347. https://doi.org/10.2903/j.efsa.2011.2347
8. Waizenegger W, Atzpadin N, Schreer O, Feldmann I, Eisert P. Model based 3D gaze estimation for provision of virtual eye contact. 2012. (ICIP-2012). Orlando Florida, USA. https://doi.org/10.1109/icip.2012.6467274
9. Bakhiya N, Appel KE. Toxicity and carcinogenicity of furan in human diet. *Archive. Toxi*. 2010;84:563–578. https://doi.org/10.1007/s00204-010-0531-y
10. Kitaev YP, Buzykin B I, Troepol'skaya T V. The review surveys the present state of research on the conformation, isomerism, and intramolecular interactions of molecules of the immense class of organic compounds containing a hydrazone group. A list of 221 references is included. *Russ. Chem. Rev*. 1970;39:441–456.
11. Belskaya NP, Dehaen W, Bakulev VA. Synthesis and properties of hydrazones bearing amide, thioamide and amidine functions. *Archive. Org. Chem*. 2010:275–332. https://doi.org/10.3998/ark.5550190.0011.108
12. Dadiboyena S, Nefzi A. Synthesis of functionalized tetrasubstituted pyrazolyl heterocycles – a review. *Eur. J. Med. Chem*. 2011;46:5258–5257. https://doi.org/10.1016/j.ejmech.2011.09.016

13. Wu AM, Senter PD. Arming antibodies: prospects and challenges for immune conjugates. *Nat. Biotechnol*. 2005;23:1137–1146.
14. Ramesh Babu N, Subashchandrabose S, Syed Ali Padusha M, Saleem H, Erdogdu Y. Synthesis and spectral characterization of hydrazone derivative of furfural using experimental and DFT methods. *Spectrochim. Acta A*. 2014;120:314–322. https://doi.org/10.1016/j.saa.2013.09.089
15. Narayan Vijay, Mishra Hriday Narayan, Prasad Onkar, Sinha Leena. Electronic structure, electric moments and vibrational analysis of 5-nitro-2-furaldehyde semicarbazone: A D.F.T. study. *Comp. Theo. Chem*. 2011;973:20–27. https://doi.org/10.1016/j.comptc.2011.06.023
16. Nathiya A, Saleem H, Bharanidharan S, Suresh M, Padusha M S A. *Int. Lrs of Chem*. 2015;61:162–177.
17. Frisch MJ, Trucks GW, Schlegel HB, Scuseria GE, Robb MA, Cheeseman JR, Montgomery JA, Vreven T, Kudin K N, Burant JC, Millam JM, Iyengar S S, Tomasi J, Barone V, Mennucci B, Cossi M, Scalmani G, Rega N, Petersson GA, Nakatsuji H, Hada M, Ehara M, Toyota K, Fukuda R, Hasegawa J, Ishida M, Nakajima T, Honda Y, Kitao O, Nakai H, Klene M, Li X, Knox JE, Hratchian H P, Cross JB, Adamo C, Jaramillo J, Gomperts R, Stratmann RE, Yazyev O, Austin A J, Cammi R, Pomelli C, Ochterski J W, Ayala P Y, Morokuma K, Voth A, Salvador P, Dannenberg J J, Zakrzewski V G, Dapprich S, Daniels A D, Strain M C, Farkas O, Malick D K, Rabuck AD, Raghavachari K, Foresman J B, Ortiz J V, Cui Q, Baboul A G, Clifford S, Cioslowski J, Stefanov B B, Liu G, Liashenko A, Piskorz P, Komaromi I, Martin R L, Fox D J, Keith T, Al-Laham M A, Peng C Y, Nanayakkara A, Challacombe M, Gill PMW, Johnson B, Chen W, Wong M W, Gonzalez C, Pople J A. Wallingford, CT: Gaussian Inc; 2004.
18. Schlegel HB. Optimization of equilibrium geometries and transition structures. *J.Comput. Chem*. 1982;3:214–218. https://doi.org/10.1002/jcc.540030212
19. Jamróz MH. *J. Mol. Struct*. 2006;787:172–183.
20. Michalska D. *Raint Program*. 2003. Wroclaw University of Technology.
21. Michalska D, Wysokinski R. *Chem. Phys. Lett*. 2005;403:211–217.
22. Ravikumar C, Joe IH, Jayakumar VS. Charge transfer interactions and nonlinear optical properties of push–pull chromophore benzaldehyde phenylhydrazone: A vibrational approach. *Chem. Phy. Lett*. 2008;460:552–558. https://doi.org/10.1016/j.cplett.2008.06.047
23. Song MZ, Fan CG. (E)-N'-(2-Furylmethylene) benzohydrazide. *Acta Cryst. E*. 2009;65:o2800.
24. Tang CB. 2-Methyl-N'-[1-(2-pyridyl) ethylidene] benzohydrazide. *Acta Cryst. E*. 2011;67:o271–o271.
25. Nair N, Sithambaresan M, Kurup M R P. N′-[(E)-(3-Fluoropyridin-2-yl) methylidene] enzohydrazide monohydrate. *Acta cryst, E*. 2012;68:2709–2709.
26. Silverstein RM, Bassler GC, Morrill TC. *Spectrometric Identification of Organic Compounds*. Chichester: John Wiley; 1991.
27. Socrates G. *Infrared and Raman Characteristic Group Frequencies–Tables and Charts*. third ed. New York: Wiley; 2001.
28. Rastogi VK, Palafox MA, Tanwar RP, Mittal L. 3,5-Difluorobenzonitrile: ab initio calculations FTIR and Raman spectra. *Spectrochim. Acta A*. 2002;58:1987–2004. https://doi.org/10.1016/s1386-1425(01)00650-3
29. Silverstein M, Basseler GC, Morill C. *Spectrometric Identification of Organic Compounds*. New York: Wiley; 1981.
30. Iliescu T, Irimie FD, Bolboaca M, Paisz Cs, Kiefer W. Vibrational spectroscopic investigations of 5-(4-fluoro-phenyl)-furan-2-carbaldehyde. *Vib. Spectrosc*. 2002;29:235–239. https://doi.org/10.1016/s0924-2031(01)00182-5
31. Socrates G. *Infrared Characteristic Group Frequencies*. New York: Wiley; 1980.
32. Varsanyi G. *Vibrational Spectra of Benzene Derivatives*. New York: Academic Press; 1969.
33. Balachandran V, Santhi G, Karpagam V, Lakshmi A. DFT computation and spectroscopic analysis of N-(p-methoxybenzylidene) aniline, a potentially useful NLO material. *J. Mol. Struct*. 2013;1047:249–261. https://doi.org/10.1016/j.molstruc.2013.05.021
34. Subramanian N, Sundaraganesan N, Jayabharathi J. Molecular structure, spectroscopic (FT-IR, FT-Raman, NMR, UV) studies and first-order molecular hyperpolarizabilities of 1,2-bis(3-methoxy-4-hydroxybenzylidene)hydrazine by density functional method. *Spectrochim. Acta A*. 2010;76:259–269. https://doi.org/10.1016/j.saa.2010.03.033

35. Roeges N P G. *A Guide to the Complete Interpretation of Infrared Spectra of Organic Structures*. New York: Wiley; 1994.
36. Barathes M, Nunzio GD, Ribet M. Polarrons or Proton transfer in chains of peptide gropus. *Synth. Met*. 1996;76:337–340.
37. Krishnakumar V, Muthunatesan S. FT-IR, FT-Raman spectra and scaled quantum mechanical study of 2,3-dihydroxy pyridine and 2,4-dihyroxy-3-nitropyridine. *Spectrochim. Acta A*. 2006;65:818–825. https://doi.org/10.1016/j.saa.2005.12.039
38. Lorenc J. *Vib. Spectrosc*. 2012;61:112–123.
39. Heckle WA, Ory HA, Talbert JM. The infrared spectra of some chlorinated derivatives of s-triazine. *Spectrochim. Acta*. 1961;17:600–606. https://doi.org/10.1016/0371-1951(61)80120-3
40. Ramesh babu N, Subashchandrabose S, Padusha MSA, Saleem H, Manivannan V, Erdogdu Y. *J.Mol. Structure*. 2014;1072:84–93.
41. Murray JS, Sen K. *Molecular Electrostatic Potentials, Concepts and 399 Applications*. Amsterdam: Elsevier; 1996.
42. Scrocco E, Tomasi J, Lowdin P. *Advances in Quantum Chemistry*. New York: Academic Press; 1978.
43. Ott JB, Goates JB. *Calculations from Statistical Thermodynamics*. Academic Press; 2000.

Publisher's Note

All claims, opinions, data, and conclusions expressed in this article are solely those of the author(s) and contributor(s), and do not necessarily represent those of Open Access Pub, the journal, its editors, or reviewers. Open Access Pub does not guarantee or endorse any product, method, instruction, or claim discussed in the article, and disclaims responsibility for any injury to people or property resulting from ideas, methods, instructions, or products referred to in the content.